Recombination of Lophyl Radicals in Pyrrolidinium-Based Ionic Liquids

Stefan Berdzinski, Joachim Horst, Petra Straßburg, and Veronika Strehmel*[a]

The recombination of photolytically generated lophyl radicals has been investigated by UV/Vis spectroscopy in 1-alkyl-1-methylpyrrolidinium bis(trifluoromethylsulfonyl)imides (NTf$_2$) in comparison with 1-butyl-3-methylimidazolium NTf$_2$, dimethyl sulfoxide, and triacetin. The 1-alkyl-1-methylpyrrolidinium-based ionic liquids contain an alkyl substituent varying between butyl and decyl groups. Optically pure ionic liquids are used in these studies. Temperature-dependent investigation of lophyl radical recombination shows an increase in the radical recombination rate with increasing temperature in each solvent, which is caused by decreasing viscosity with increasing temperature. Furthermore, the viscosity of the 1-alkyl-1-methylpyrrolidinium NTf$_2$ increases nearly linearly within the row of these ionic liquids. In contrast, the recombination of the pho-

tolytically generated lophyl radicals is significantly faster in the ionic liquids than in the traditional organic solvents under investigation. Moreover, the recombination rate increases with the length of the alkyl chain bound at the cation of the ionic liquid at a given temperature. This may be caused by an increase in the extent of lophyl radical recombination within the solvent cage. Solvent cage effects dominate in the case of lophyl radical recombination in ionic liquids bearing a long alkyl chain or if the temperature is near the melting temperature of the ionic liquid. The positive value of the activation entropy supports this hypothesis. The results obtained are important for discussion of bimolecular radical reactions in ionic liquids.

1. Introduction

Hexaarylbisimidazole (HABI) and its derivatives have been of interest in academic research[1–3] and for practical applications[4] for half a century. Their function as polymerization initiator in photoinduced polymerization systems represents one example of their use.[4, 5] Although some HABI derivatives undergo thermal dissociation into two radicals, the o-chloro-substituted HABI derivative is thermally stable at elevated temperatures, that is, even at 80 °C.[1l]

Irradiation of HABI derivatives with light results in the formation of lophyl radicals that recombine in the dark.[1a,h,j,l,y, 2e,h,i,k] The lophyl radicals formed exhibit a purple color in the reaction medium. These radicals were detected by the appearance of a bathochromic shifted absorption band in the UV/Vis spectrum[1j,k,o] and by ESR spectroscopy.[1b,q,y] Furthermore, lophyl radicals are relatively stable in air-saturated surroundings.[1l] Moreover, recombination of lophyl radicals occurs very slowly relative to other radicals formed by photolysis of a photoinitiator. It strongly depends on the substituent pattern of the HABI derivative on the one hand and on the surroundings on the other hand. The latter can be a solvent, a low-molecular-weight organic matrix, an ionic liquid, or a glassy polymer.[1i-l,y, 2e,h,i, 3] The viscosity of the surrounding matrix and, therefore, the mobility of the lophyl radicals can be varied in a broad

range to examine the recombination dynamics of the lophyl radicals in the surroundings. Recently, investigation of lophyl radicals has become of interest in ionic liquid research because they are new solvents and materials with high application potential for various processes, including those that occur through a radical mechanism.[3, 6] This allows one to draw conclusions about dynamic processes based on cage systems. Thus, the lophyl radicals are useful intermediates to develop models describing the reactivity of radicals in such matrices.

Ionic liquids are distinguished from traditional solvents because they are composed of ions. Therefore, ionic interactions are very important beside hydrogen-bonding and van der Waals interactions in the case of ionic liquids. The structure of ionic liquids can be broadly varied by variation of the combination of various cations and anions. This results in a broad variation of the physical properties, such as melting behavior, viscosity, and polarity, of these tailor-made designer solvents.[7] Therefore, ionic liquids are interesting matrices for investigation of lophyl radicals. Previous investigation on lophyl radical recombination in imidazolium-based ionic liquids showed a significantly faster recombination reaction of the lophyl radicals in these ionic liquids than expected from their macroscopic viscosity.[3a] This was attributed to solvent cage effects in the ionic liquids that are different from those in molecular solvents.

Herein, we discuss lophyl radical recombination in 1-alkyl-1-methylpyrrolidinium bis(trifluoromethylsulfonyl)imides in comparison with 1-butyl-3-methylimidazolium bis(trifluoromethylsulfonyl)imide (BuMImNTf$_2$), dimethyl sulfoxide (DMSO), and tri-

[a] S. Berdzinski, J. Horst, P. Straßburg, Prof. Dr. V. Strehmel
Hochschule Niederrhein, University of Applied Sciences
Department of Chemistry
Organic Chemistry and Institute for Coatings and Surface Chemistry
Adlerstraße 32, 47798 Krefeld (Germany)
E-mail: veronika.strehmel@hsnr.de

acetin as a function of temperature to determine the activation parameters for radical recombination in the dark; these are the activation enthalpy and activation entropy. The latter allows drawing of conclusions about the steric requirements on the transition state in a bimolecular process, which should be negative. Furthermore, the alkyl chain of the pyrrolidinium bis(trifluoromethylsulfonyl)imides varies between butyl and decyl groups resulting in variation of both viscosity and polarity.[8] The BuMImNTf$_2$ and the organic solvents are lower in viscosity than the pyrrolidinium bis(trifluoromethylsulfonyl)imides.[8–11] Furthermore, solvent cage effects may be different in these solvents as well. Moreover, optically pure ionic liquids were used for the irradiation experiments to avoid absorption of light by the ionic liquid at the wavelength used for the irradiation experiments (365 nm).

2. Results and Discussion

2.1. Solvent Properties

Commercially available ionic liquids often exhibit a colored appearance, which can sometimes be slightly yellow or brown. Even if they are colorless they may show a small absorption at 365 nm, which is the irradiation wavelength used in our experiments. General cleaning procedures published in the literature focus on the use of adsorbents, such as charcoal, silica gel, or aluminum oxide.[12a] Although the ionic liquids become colorless by purification using these adsorbents, trace amounts of the adsorbents may remain in the ionic liquids resulting in new impurities.[12b] The influence of these new impurities on the formation and recombination of lophyl radicals is not yet known. Our extensive purification procedure (see the Experimental Section) yields optically pure ionic liquids that possess a significantly higher optical purity than commercially available materials.

The solvents investigated in this work are 1-alkyl-1-methyl-pyrrolidinium bis(trifluoromethylsulfonyl)imides, BuMImNTf$_2$, DMSO, and triacetin (Scheme 1). The latter is an example of a higher-viscosity molecular solvent.

Excitation of 2,2′-di(ortho-chlorophenyl)-4,4′,5,5′-tetraphenylbisimidazole (o-Cl-HABI) with light results in formation of two lophyl radicals (L•) as shown in Scheme 2. The irradiation experiments were carried out at 365 nm with a Hg(Xe) lamp in combination with an interference filter. This gives reliable results compared with the previous laser flash photolysis studies.[3a]

After formation of the lophyl radicals they can recombine within the solvent cage or they can escape out of the solvent cage, diffuse through the matrix, and recombine with another lophyl radical resulting in back formation of the dimer (Scheme 2). The solvent cage may differ for the solvents investigated in this work, and the lophyl radical recombination reaction may be used to probe these differences in the solvent cage between ionic liquids and molecular solvents.

The ionic liquids and molecular solvents under investigation possess different viscosities (Table 1).[9–11] DMSO shows the lowest viscosity in this row and is followed by triacetin and BuMImNTf$_2$. All pyrrolidinium bis(trifluoromethylsulfonyl)imides are higher-viscosity solvents, and their viscosity increases with the length of the alkyl chain bound at the nitrogen atom of the pyrrolidinium ring, from the butyl group to the decyl substituent (Table 1). Furthermore, the polarity also differs for these solvents.[8a,b, 13]

Scheme 1. Structures of 1-alkyl-1-methylpyrrolidinium bis(trifluoromethylsulfonyl)imides (alkyl = butyl, pentyl, hexyl, heptyl, octyl, nonyl, decyl), 1-butyl-3-methylimidazolium bis(trifluoromethylsulfonyl)imide (BuMImNTf$_2$), dimethyl sulfoxide (DMSO), and glycerin triacetate (triacetin).
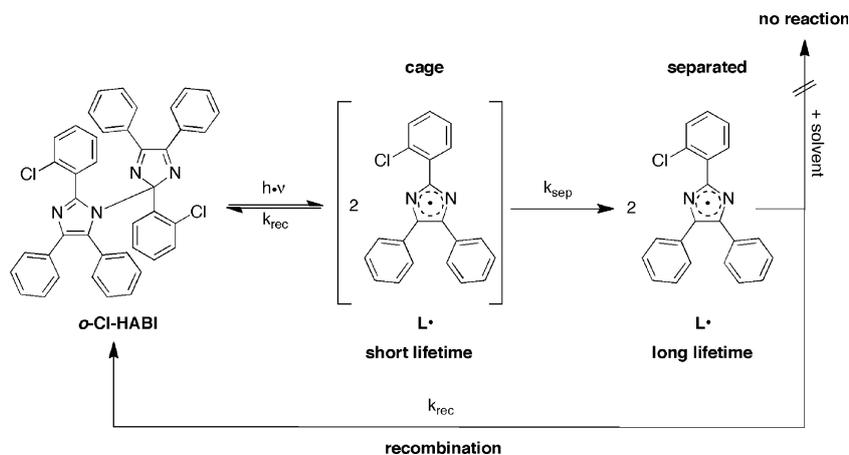
Scheme 2. Reaction scheme for light-induced formation of lophyl radicals (L•) and their recombination within the solvent cage or reaction with another lophyl radical after escape out of the solvent cage and diffusion through the matrix.[1v] k_{rec} = rate constant for radical recombination; k_{sep} = rate constant for radical separation.

Table 1. Viscosity (η) of ionic liquids and molecular solvents used for excitation of o-Cl-HABI at 297 K, which results in formation of L⁻ having a wavelength maximum (λ_{max}), and rate constant for recombination of lophyl radicals (k_{rec}) at 297 K.

Solvent	η [mPa s]	λ_{max} [nm]	k_{rec} [L mol⁻¹ s⁻¹]
BuMPyrNTf₂	86	553	1991
PentMPyrNTf₂	108	558	2235
HexMPyrNTf₂	119	558	2311
HepMPyrNTf₂	135	556	2449
OctMPyrNTf₂	156	554	2605
NonMPyrNTf₂	185	557	2911
DecMPyrNTf₂	194	557	9699
BuMImNTf₂	40[3a, 9]	541	2732
DMSO	2[10]	561	401
triacetin	16[11]	553	712

Figure 1. Absorption spectra of lophyl radicals in selected solvents: 1: BMPyrNTf₂, 2: DecMPyrNTf₂, 3: BuMImNTf₂, 4: DMSO, and 5: triacetin (see legend). OD = optical density.

2.2. Absorption of Lophyl Radicals

Although the absorption maximum of o-Cl-HABI is below 300 nm it exhibits a long absorption tail covering the exposure wavelength at 365 nm. Most of the ionic liquids do absorb at the absorption maximum of the o-Cl-HABI as well.[1l,r] Therefore, 365 nm was chosen as the wavelength for our irradiation experiments because the purified ionic liquids exhibit an open optical window at this wavelength. Irradiation of o-Cl-HABI at 365 nm results in formation of two lophyl radicals (L⁻) as described in Scheme 2. The lophyl radicals formed show a new absorption band (Figure 1) in the visible region. The absorption maximum is between 553 and 561 nm depending on the solvent used (Table 1). Furthermore, optical densities of the lophyl radicals measured after excitation until the equilibrium is reached differ for the solvents investigated, although the same concentration of o-Cl-HABI was used for the experiments (Figure 1). The lowest optical density is observed for the lophyl radicals in DecMPyrNTf₂, although the optical density of lophyl radicals is similar in DMSO and in the other ionic liquids. This gives a slight hint for differences in lophyl radical recombination in these solvents.

2.3. Dimerization Kinetics of Lophyl Radicals at 297 K

Investigation of dimerization kinetics was carried out at 297 K, that is, near room temperature. Lophyl radicals were generated by irradiation of o-Cl-HABI in solution until the equilibrium of lophyl radical concentration was reached. The optical densities of the lophyl radicals are plotted as a function of time during the radical recombination reaction

in the dark (Figure 2). The fastest decay of lophyl radicals is observed in the ionic liquids, whereas the slowest decay of lophyl radicals is found in DMSO. Furthermore, the decay of the lophyl radicals is faster in triacetin than DMSO and slower relative to the ionic liquids. Recombination of lophyl radicals can be described as a second-order reaction by using Equation (1):

$$\frac{1}{OD(t)} = \frac{1}{OD_0 \, \varepsilon \, d} + \frac{2 k_{rec}}{\varepsilon \, d} \cdot t \tag{1}$$

in which OD(t) is the optical density of the lophyl radicals as a function of time (t), OD₀ is the optical density of the lophyl radicals after irradiation with light at 365 nm until the equilibri-
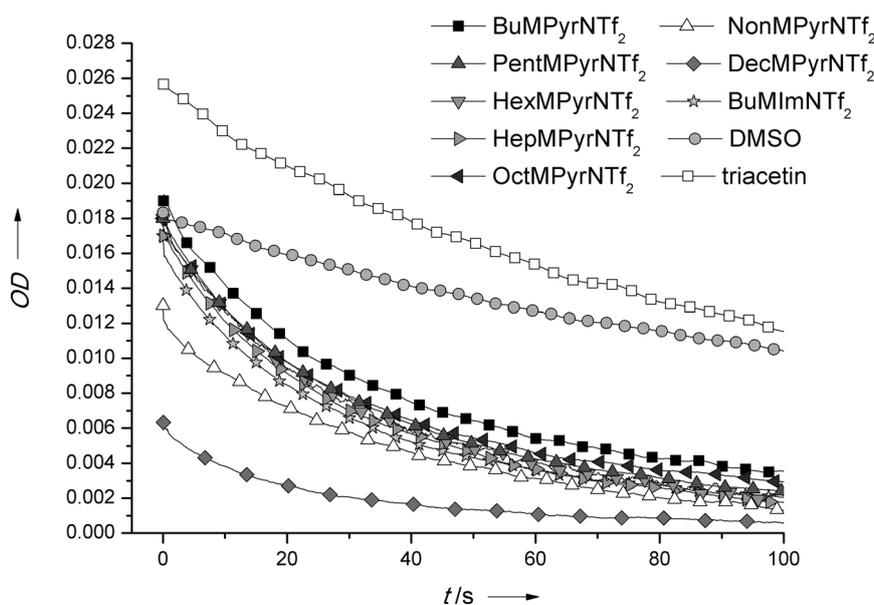
Figure 2. Optical density of lophyl radicals at λ_{max} (see Table 1) as a function of time (t) during the dark reaction in BuMPyrNTf₂, PentMPyrNTf₂, HexMPyrNTf₂, HepMPyrNTf₂, OctMPyrNTf₂, NonMPyrNTf₂, DecMPyrNTf₂, BuMImNTf₂, DMSO, and triacetin at 297 K.

um at the beginning of the dark reaction, ε is the extinction coefficient of the lophyl radicals, d is the layer thickness, and k_{rec} is the rate constant for lophyl radical recombination. The second-order rate constants calculated by using Equation (1) are summarized in Table 1. The rate constants are significantly higher in the ionic liquids in comparison with the molecular solvents triacetin and DMSO. Furthermore, the rate constants for dimerization increase within the row of the 1-alkyl-1-methylpyrrolidinium salts with increasing viscosity. The rate constants for lophyl radical recombination increase linearly with the viscosity from the butyl- up to the nonyl-substituted pyrrolidinium-based ionic liquids (Figure 3). Moreover, the rate con-
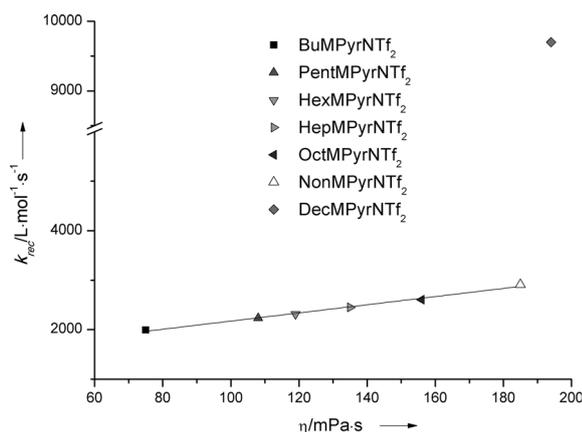
Figure 3. Viscosity (η) dependence of the rate constant for lophyl radical recombination (k_{rec}) at 297 K for 1-alkyl-1-methylpyrrolidinium bis(trifluoromethylsulfonyl)imides bearing butyl, pentyl, hexyl, heptyl, octyl, nonyl, or decyl substituents.

stant for dimerization is significantly higher in the high-viscosity ionic liquids than in triacetin. Furthermore, only a small drop of k_{rec} is observed by switching to the much lower viscosity DMSO. These results show that the rate constant for lophyl radical recombination is higher if the solvent viscosity is higher. This finding can be explained by a higher extent of lophyl radical recombination within the solvent cage with increasing viscosity of the matrix in the case of the pyrrolidinium-based ionic liquids. In contrast, the rate constant for lophyl radical recombination is higher in the butyl-substituted imidazolium salt than in the pyrrolidinium salt bearing similar substituents, and is significantly higher relative to the molecular solvents although the viscosity of the molecular solvents is significantly lower. These examples show that lophyl radical recombination is a complex process that is influenced by the solvent viscosity and by solvent cage effects. Moreover, the use of DecMPyrNTf$_2$ results in the highest rate constant for lophyl radical recombination, which locates outside the expected viscosity trend (Figure 3). This may be caused by the melting point of the DecMPyrNTf$_2$ of 286 K, which is only 11 K below the temperature used for investigation of lophyl radical recombination. Mobility investigation of stable radicals in ionic liquids shows that the radicals are strongly immobilized near the melting point.[14] This gives a first hint that diffusion through the matrix may be strongly reduced at 297 K, which is only

11 K above the melting point of the DecMPyrNTf$_2$, and therefore the radicals may recombine within the solvent cage to a significantly higher extent at 297 K in this ionic liquid.

As described in Scheme 2, two processes of recombination can be discussed: recombination within the solvent cage, and recombination after escape out of the solvent cage and diffusion through the matrix. The results summarized in Table 1 and Figure 2 show the complexity of lophyl radical recombination. Solvent cage effects exhibit a higher dominance either in very viscous media or near the melting point of the matrix because diffusion is strongly limited under such conditions. Furthermore, solvent cage effects may become more dominant if the length of the alkyl substituent at the pyrrolidinium ion increases. The increase in the alkyl chain length at the pyrrolidinium ion results in an increase in viscosity of the pyrrolidinium bis(trifluoromethylsulfonyl)imides. The higher extent of in-cage lophyl radical recombination may explain the increase in the rate constant of lophyl radical recombination with increasing viscosity of the pyrrolidinium bis(trifluoromethylsulfonyl)imides (Figure 3). Moreover, solvent cage effects and lophyl radical recombination after their diffusion through the ionic liquid may also differ between BuMPyrNTf$_2$ and BuMImNTf$_2$. The higher rate constant for lophyl radical recombination in the case of the BuMImNTf$_2$ compared to BuMPyrNTf$_2$ may be explained by the lower viscosity of the BuMImNTf$_2$ that results in faster diffusion of lophyl radicals through the ionic liquid on the one hand, and by stronger solvent cage effects caused by the aromatic structure on the other hand.

The results of lophyl radical recombination summarized in Table 1 and depicted in Figure 3 lead to the conclusion that both solvent viscosity and solvent cage effects influence the radical recombination in the dark. Furthermore, investigation of the temperature dependence of lophyl radical recombination helps us to understand the influence of viscosity and solvent cage effects on the lophyl radical recombination reaction.

2.4. Dimerization Kinetics of Lophyl Radicals at Different Temperatures

Lophyl radical recombination was investigated in ionic liquids and molecular solvents in the temperature range between 283 and 343 K. In the case of the decyl-substituted 1-alkyl-1-methylpyrrolidinium bis(trifluoromethylsulfonyl)imide, a temperature region between 283 and 303 K was selected for investigation of lophyl radical recombination because radical recombination was too fast to follow with our experimental setup outside of this temperature window in the case of this ionic liquid. Furthermore, a temperature window between 283 and 323 K was used for investigation of radical recombination in 1-nonyl-1-methylpyrrolidinium bis(trifluoromethylsulfonyl)imide for the same reason. The use of the Eyring equation [Eq. (2)] yields the necessary information about activation enthalpy ($\Delta H^{\neq}$) and activation entropy ($\Delta S^{\neq}$):

$$\ln \frac{k_{rec}}{T} = \ln \frac{k_B}{h} + \frac{\Delta S^{\neq}}{R} - \frac{\Delta H^{\neq}}{R} \cdot \frac{1}{T} \qquad (2)$$

in which k_{rec} is the rate constant of radical recombination, T the temperature, k_B the Boltzmann constant, h the Planck constant, and R the gas constant.

The Eyring plots are depicted in Figure 4 for all solvents investigated. These plots well describe the temperature dependence of the lophyl radical recombination. As expected, the rate
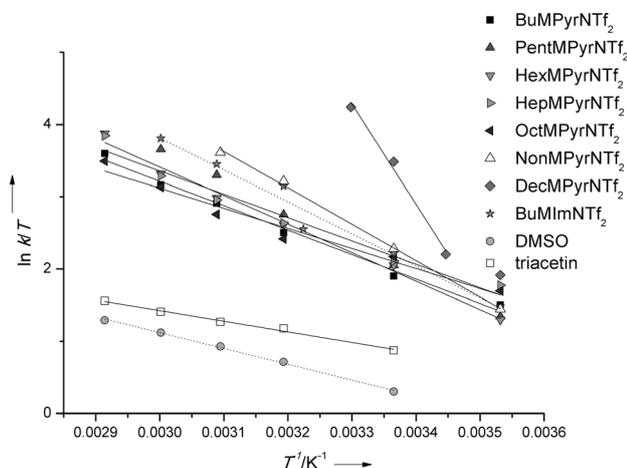
Figure 4. Eyring plots for lophyl radical recombination in ionic liquids (BuM-PyrNTf$_2$, PentMPyrNTf$_2$, HexMPyrNTf$_2$, HepMPyrNTf$_2$, OctMPyrNTf$_2$, Non-MPyrNTf$_2$, DecMPyrNTf$_2$, BuMImNTf$_2$) and molecular solvents (DMSO, triacetin).

constants for lophyl radical recombination increase with increasing temperature in the case of all solvents investigated. This is caused by the decrease in the viscosity of the solvents with increasing temperature, which results in faster diffusion of the radicals and, therefore, in higher rate constants for radical recombination. The activation enthalpies of lophyl radical recombination and the activation energy for the viscous flow of the ionic liquids are summarized in Table 2. The activation energy for the viscous flow of the 1-alkyl-1-methylpyrrolidinium bis(trifluoromethylsulfonyl)imides and the activation enthalpy for lophyl radical recombination in these ionic liquids

are similar for the pyrrolidinium salts substituted by a butyl up to an octyl group. This shows a controlled recombination in the microscopic domain with the viscosity as macroscopic parameter. A slightly higher activation enthalpy of lophyl radical recombination is observed for the nonyl-substituted pyrrolidinium salt. Furthermore, the decyl-substituted pyrrolidinium salt exhibits significantly higher values for both the activation energy of the viscous flow and the activation enthalpy of lophyl radical recombination. The higher values obtained for the decyl-substituted pyrrolidinium bis(trifluoromethylsulfonyl)imide indicate that the activation enthalpy for the structural reorganization of the lophyl radicals may influence significantly the radical recombination process. Furthermore, activation parameters for lophyl radical recombination in the decyl-substituted pyrrolidinium salt were not investigated at a temperature higher than 303 K, because radical recombination was too fast in this ionic liquid to be measured with our experimental setup.

Moreover, the activation enthalpy is slightly higher for the imidazolium bis(trifluoromethylsulfonyl)imide than the pyrrolidinium-based ionic liquids bearing a short alkyl group and the same anion. This shows that the temperature has a stronger effect on radical recombination in the case of the imidazolium salt relative to the pyrrolidinium salts substituted with a short alkyl group. Comparison of the activation energy for the viscous flow (E_η) of the ionic liquids with the activation enthalpy for radical recombination ($\Delta H^{\ddagger}$) leads to the conclusion that self-diffusion of the matrix and radical recombination show a similar temperature dependence in most ionic liquids except the decyl-substituted pyrrolidinium salt.[1v, 15] However, radical recombination is less temperature dependent in the case of the molecular solvents DMSO and triacetin, although triacetin is also highly viscous. The higher activation energy obtained for radical recombination in the ionic liquids may be attributed to the ionic interactions between the cation and the anion of the ionic liquid, which are absent in the molecular solvents.

Additional information can be observed from the activation entropy ($\Delta S^{\ddagger}$) for lophyl radical recombination, which is negative for most examples. This indicates a high steric requirement on the transition state in the case of molecular solvents and most ionic liquids investigated. The most negative activation entropies were found for the molecular solvents. This indicates that radical recombination after escape out of the solvent cage and diffusion through the matrix may be dominant in the organic solvents. The value obtained is typical for a bimolecular reaction with a large steric requirement on the transition state. The less negative value for the activation entropy obtained for radical recombination in the ionic liquids leads to the conclusion that radical recombination within the solvent cage may play a greater role in the case of radical recombination in ionic liquids and that the steric requirements are not as large as those for traditional solvents. The positive activation entropies obtained for radical recombination in NonMPyrNTf$_2$ and DecM-PyrNTf$_2$ show that radical recombination within the solvent cage occurs to a significantly higher extent relative to the other ionic liquids, because radical recombination within the solvent cage does not necessitate such a high steric require-

Table 2. Activation energy for the viscous flow (E_η) of the solvents in the temperature range (T_1–T_2). Activation enthalpy ($\Delta H^{\ddagger}$) and entropy ($\Delta S^{\ddagger}$) for lophyl radical recombination determined from measurements in BuM-PyrNTf$_2$, PentMPyrNTf$_2$, HexMPyrNTf$_2$, HepMPyrNTf$_2$, OctMPyrNTf$_2$, DMSO, and triacetin at 283, 297, 313, 324, 333, and 343 K, in NonMPyrNTf$_2$ at 283, 290, 297, and 303 K, and in DecMPyrNTf$_2$ at 283, 297, 313, and 324 K using Equation (2).

Solvent	E_η [kJ mol^{-1}]	$\Delta H^{\ddagger}$ [kJ mol^{-1}]	$\Delta S^{\ddagger}$ [J mol^{-1} K^{-1}]
BuMPyrNTf$_2$	29 (23–70 °C)	28	−86
PentMPyrNTf$_2$	29 (23–70 °C)	31	−78
HexMPyrNTf$_2$	29 (23–70 °C)	33	−71
HepMPyrNTf$_2$	30 (23–70 °C)	27	−89
OctMPyrNTf$_2$	26 (23–70 °C)	23	−102
NonMPyrNTf$_2$	31 (23–70 °C)	42	20
DecMPyrNTf$_2$	68 (23–70 °C)	115	219
BuMImNTf$_2$	24[9]	39	−52
DMSO	13[10]	18	−133
triacetin	45 (−5−+35 °C)[11]	12	−149

ment on the transition state as for the case in which radicals escape out of the solvent cage, diffuse through the matrix, and meet another radical for the recombination reaction.

3. Conclusions

The faster lophyl radical recombination in ionic liquids in comparison with molecular solvents and the differences in the rate constants for lophyl radical recombination between the single ionic liquids indicate differences in the solvent cage between ionic liquids and molecular solvents on the one hand, and between ionic liquids bearing a variation of the alkyl chain length on the other hand. In contrast, the rate constant for lophyl radical recombination increases with temperature in the case of each individual solvent. This is caused by a decrease in the viscosity with increasing temperature. From this one can conclude that measurements as a function of temperature give information only about the influence of the solvent viscosity on lophyl radical recombination keeping the solvent cage constant. A variation of the solvent structure may result in differences in the solvent cage. Therefore, both the viscosity of the solvent and solvent cage effects influence the rate constant for lophyl radical recombination in the case of different solvents at the same temperature.

Furthermore, the more negative values for the activation entropy determined from temperature-dependent measurements in the molecular solvents indicate higher steric requirements on the transition state in the molecular solvents relative to the ionic liquids. From this one can conclude that lophyl radical recombination occurs after escape of lophyl radicals out of the solvent cage and diffusion through the matrix to a higher extent than in the case of ionic liquids. The less negative values for the activation entropy for lophyl radical recombination in the case of most ionic liquids indicate a higher extent of lophyl radical recombination within the solvent cage. The positive values for the activation entropy for lophyl radical recombination in NonMPyrNTf$_2$ and DecMPyrNTf$_2$ indicate a higher extent of lophyl radical recombination within the solvent cage. From this one can conclude that the concentration of radicals that escape out of the solvent cage strongly differs between ionic liquids and molecular solvents. Therefore, reactions of two radicals that are formed from one radical precursor may be strongly influenced by solvent cage effects in the ionic liquids. This may be important, for example, for the understanding of free-radical polymerization reactions in ionic liquids and the influence of ionic liquids on the molecular weight of the polymers obtained, which is mostly higher if the polymerization is carried out in ionic liquids rather than molecular solvents.

Experimental Section

Materials

The 2,2′-di(*ortho*-chlorophenyl)-4,4′,5,5′-tetraphenylbisimidazole (*o*-Cl-HABI) was available as a commercial compound, and was used without further purification. All starting materials, such as 1-chloro-butane (Sigma–Aldrich), 1-chloropentane (Sigma–Aldrich), 1-chloro-hexane (Sigma–Aldrich), 1-chloroheptane (Sigma–Aldrich), 1-chlorooctane (Sigma–Aldrich), 1-chlorononane (Sigma–Aldrich), 1-chlorodecane (Sigma–Aldrich), 1-methylpyrrolidine (Sigma–Aldrich), isopropanol (Carl Roth), ethyl acetate (Carl Roth), dichloromethane (Carl Roth), acetone (Carl Roth), acetonitrile (Carl Roth), and water, were distilled before use. Lithium bis(trifluoromethylsulfonyl)imide was purchased from IoLiTec and used as received.

For simplicity of substance names, acronyms are used to describe the cations: Pyr = pyrrolidinium, Im = imidazolium, for the attached alkyl group M = methyl, Bu = butyl, Pent = pentyl, Hex = hexyl, Hep = heptyl, Oct = octyl, Dec = decyl; for example, BuMPyr corresponds to *N*,*N*-butylmethylpyrrolidinium cation.

Synthesis and Purification Procedure of the *N*,*N*-Alkylmethylpyrrolidinium Chlorides

All synthesis and purification steps were carried out under exclusion of visible and UV light. Furthermore, the alkylation of *N*-methylpyrrolidine was carried out with alkyl chloride in a nitrogen atmosphere. The white to slightly yellow or slightly brown colored *N*-alkyl-*N*-methylpyrrolidinium chlorides obtained were extracted with ethyl acetate by using the *N*-alkyl-*N*-methylpyrrolidinium chloride as stationary phase in column chromatography. The impurities were extracted efficiently with ethyl acetate. Extraction was continued until the *N*-alkyl-*N*-methylpyrrolidinium chloride did not show any absorption at 365 nm, which is the excitation wavelength for the chromophore under investigation. Finally, the *N*-alkyl-*N*-methylpyrrolidinium chlorides were recrystallized using a mixture of acetonitrile and ethyl acetate.

BuMPyrNTf$_2$

N-Methylpyrrolidine (139.7 g, 1.63 mol) was dissolved in isopropanol (170 mL) and 1-chlorobutane (161.2 g, 1.74 mol) was added dropwise at 3 °C for 2 h. After the reaction mixture was stirred for 24 h at 82 °C, it was cooled to room temperature. The solid BuMPyrCl was dried and transferred into a column used for column chromatography. Extraction of BMPyrCl was carried out with ethyl acetate (2 L) at one drop per 4 s dropping rate. The extracted BuMPyrCl was further purified by recrystallization using ethyl acetate/acetonitrile (vol/vol = 1:6.7) followed by further washing with ethyl acetate (200 mL) and drying in vacuo. Yield: 80 % (231.4 g, 1.30 mol); m.p. 207–209 °C; ^{1}H NMR (300 MHz, D$_2$O, 25 °C, TMS): δ = 3.60–3.32 (m, 4H; CH$_2$), 3.36–3.18 (m, 2H; CH$_2$), 2.97 (s, 3H; CH$_3$), 2.14 (s, 4H; CH$_2$), 1.86–1.59 (m, 2H; CH$_2$), 1.49–1.20 (m, 2H; CH$_2$), 0.89 ppm (t, ^3J(H,H) = 7.4 Hz, 3H; CH$_3$); ^{13}C NMR (75 MHz, D$_2$O, 25 °C, TMS): δ = 64.4–64.2 (m; CH$_2$), 64.1–64.1 (m; CH$_2$), 48.9–47.3 (m; CH$_3$), 25.1 (CH$_2$), 21.3 (CH$_2$), 19.3 (CH$_2$), 12.88 ppm (CH$_3$); IR: $\tilde{\nu}$ = 741, 765, 788, 1050, 1224, 1325, 1342, 1464 (C-H), 2965 cm^{-1} (C-H); MS positive mode: *m/z* (%): 142 (100) [*M*$^+$], MS (35 eV): *m/z* (%): 142 (25) [*M*$^+$], 86 (100) [C$_5$H$_{12}$N$^+$].

A solution of lithium bis(trifluoromethylsulfonyl)imide (81.0 g, 280 mmol) in water (35 mL) was added under stirring to a solution of *N*,*N*-butylmethylpyrrolidinium chloride (46.5 g, 262 mmol) dissolved in water (20 mL). The reaction mixture was further stirred for 24 h at room temperature. Then, dichloromethane (120 mL) was added. The organic layer was separated and washed with water (5 × 50 mL). Subsequently, the organic layer was dried over Na$_2$SO$_4$ overnight. The solvent was removed by evaporation. The BuMPyrNTf$_2$ was dried for 24 h in vacuo at 50 °C. Yield: 86 % (95.39 g, 225 mmol), water content: 0.01 %; ^{1}H NMR (300 MHz, CD$_3$CN, 25 °C, TMS): δ = 3.46–3.41 (m, 4H; CH$_2$), 3.29–3.23 (m, 2H;

CH_2), 2.98 (s, 3H; CH_3), 2.21–2.19 (m, 4H; CH_2), 1.81–1.70 (m, 2H; CH_2), 1.48–1.31 (m, 2H; CH_2), 1.00 ppm (t, ^3J(H,H) = 7.4 Hz, 3H; CH_3); ^{13}C NMR (75 MHz, CD_3CN, 25 °C, TMS): δ = 119,9 (q, ^1J(C,F) = 320.7 Hz; CF_3), 64.2 (CH_2-N), 48.1 (CH_3-N), 28.0 (N-CH_2-CH_2), 23.0 (CH_2-CH_2-CH_3), 21.8 (CH_2-CH_3), 21.3 (CH_2), 13.1 ppm (CH_2-CH_3); IR: $\tilde{v}$ = 739, 761, 788, 927, 1133, 1226, 1329 (S=O), 1347, 1467 (C-H), 2880, 2969 cm^{-1} (C-H); MS: negative mode m/z (%): 280 (100) [M^-], 147 (24) [$CF_3NO_2S^-$]; MS (35 eV) positive mode: m/z (%): 142 (25) [M^+], 86 (100) [$C_5H_{12}N^+$]. Differential scanning calorimetry (DSC) measurements using cooling and heating rates of 5 K min^{-1} showed the glass transition temperature (T_g) at −88.4 °C, recrystallization ($T_{recryst}$) at −57.4 °C, and two endothermic peaks at −26.8 °C corresponding to solid–solid transition (T_{m1}) and at −17.1 °C corresponding to melting of the crystal structures (T_{m2}) during heating. The refractive index was 1.4224 at 25 °C and the density was 1.277 g cm^{-3} at 25 °C.

PentMPyrNTf$_2$

N-Methylpyrrolidine (252.1 g, 2.9 mol) was dissolved in isopropanol (300 mL) and 1-chloropentane (337.0 g, 3.16 mol) was added dropwise at 3 °C for 2 h. After the reaction mixture was stirred for 24 h at 82 °C, it was cooled to room temperature. The solid PentMPyrCl was dried and transferred into a column used for column chromatography. Extraction of PentMPyrCl was carried out with ethyl acetate (2 L) at one drop per 4 s dropping rate. The extracted PentMPyrCl (254.7 g) was further purified by recrystallization using ethyl acetate/acetonitrile (vol/vol = 1:0.45) followed by further washing with ethyl acetate (300 mL) and drying in vacuo. Yield: 42% (234.4 g, 1.20 mol); m.p. 175 °C; ^1H NMR (300 MHz, D_2O, 25 °C, TMS): δ = 3.52–3.32 (m, 4H; CH_2), 3.31–3.13 (m, 2H; CH_2), 2.95 (s, 3H; CH_3), 2.12 (s, 4H; CH_2), 1.75–1.69 (m, 2H; CH_2-CH_3), 1.42–1.15 (m, 4H; CH_2), 0.82 ppm (t, ^3J(H,H) = 7.4 Hz, 3H; CH_3); ^{13}C NMR (75 MHz, D_2O, 25 °C, TMS): δ = 64.3–64.2 (m; N-CH_2), 64.2–64.1 (m; N-CH_2-CH_2), 48.0–47.9 (m; N-CH_3), 27.8 (N-CH_2-CH_2), 22.7 (CH_2-CH_2-CH_3), 21.5 (CH_2, s, CH_2-CH_3), 21.3 (CH_2-CH_2), 13.0 ppm (CH_2-CH_3); IR: $\tilde{v}$ = 741, 761, 788, 1050, 1225, 1325, 1342, 1465 (C-H), 2963 cm^{-1} (C-H); MS positive mode: m/z (%): 165 (100) [M^+]; MS (35 eV): m/z (%): 156 (30) [M^+], 86 (100) [$C_5H_{12}N^+$].

A solution of lithium bis(trifluoromethylsulfonyl)imide (98.7 g, 344 mmol) in water (36 mL) was added under stirring to a solution of *N,N*-pentylmethylpyrrolidinium chloride (62.8 g, 328 mmol) dissolved in water (25 mL). The reaction mixture was further stirred for 24 h at room temperature. Then, dichloromethane (100 mL) was added. The organic layer was separated and washed with water (7 × 100 mL). Subsequently, the organic layer was dried over Na_2SO_4 overnight. The solvent was removed by evaporation. The PentMPyrNTf$_2$ was dried for 24 h in vacuo at 50 °C. Yield: 76% (108.6 g, 249 mmol), water content: 0.078%; ^1H NMR (300 MHz, CD_3CN, 25 °C, TMS): δ = 3.49–3.42 (m, 4H; CH_2), 3.29–3.23 (m, 2H; CH_2), 3.00 (s, 3H; CH_3), 2.14–2.17 (m, 4H; CH_2), 1.83–1.73 (m, 2H; CH_2), 1.48–1.26 (m, 4H; CH_2), 0.96 ppm (t, ^3J(H,H) = 6.9 Hz, 3H; CH_3); ^{13}C NMR (75 MHz, CD_3CN, 25 °C, TMS): δ = 119.9 (q, ^1J(C,F) = 320.6 Hz; CF_3), 64.2 (CH_2-N), 48.1 (CH_3-N), 28.0 (N-CH_2-CH_2), 23.0 (CH_2-CH_2-CH_3), 21.8 (CH_2-CH_3), 21.3 (CH_2), 13.1 ppm (CH_2-CH_3); IR: $\tilde{v}$ = 739, 788, 931, 1052, 1133, 1177, 1225, 1330 (S=O), 1347, 1469 (C-H), 2964 cm^{-1} (C-H); MS negative mode: m/z (%): 280 (100) [M^-], 147 (24) [$CF_3NO_2S^-$]; MS positive mode (35 eV): m/z (%): 156 (64) [M^+], 86 (100) [$C_5H_{12}N^+$]. DSC measurements using cooling and heating rates of 5 K min^{-1} showed crystallization (T_{cryst}) at −36.3 °C during cooling, and T_g at −89.2 °C, $T_{recryst}$ at −32.3 °C, and melting of the crystal structures (T_m) at 7.9 °C during heating. The

refractive index was 1.4245 at 25 °C and the density was 1.287 g cm^{-3} at 25 °C.

HexMPyrNTf$_2$

N-Methylpyrrolidine (132.2 g, 1.6 mol) was dissolved in isopropanol (125 mL) and 1-chlorohexane (200.0 g, 1.7 mol) was added dropwise at 3 °C for 1.5 h. After the reaction mixture was stirred for 24 h at 82 °C, it was cooled to room temperature resulting in precipitation of HexMPyrCl. The solid HexMPyrCl was dried and transferred into a column used for column chromatography. Extraction of HexMPyrCl was carried out with ethyl acetate (2 L) at one drop per 4 s dropping rate. The extracted HexMPyrCl was further purified by recrystallization using ethyl acetate/acetone (vol/vol = 1:1) followed by further washing with ethyl acetate (300 mL) and drying in vacuo. Yield: 53% (174.7 g, 849 mmol); m.p. 190 °C; ^1H NMR (300 MHz, D_2O, 25 °C, TMS): δ = 3.44–3.40 (m, 4H; CH_2), 3.27–3.22 (m, 2H; CH_2), 2.97 (s, 3H; CH_3), 2.23 (s, 4H; CH_2), 1.77–1.67 (m, 2H; CH_2), 1.33–1.23 (m, 6H; CH_2), 0.80 ppm (t, ^3J(H,H) = 6.7 Hz, 3H; CH_3); ^{13}C NMR (75 MHz, D_2O, 25 °C, TMS): δ = 64.34–64.38 (m, N-CH_2), 64.3–64.1 (m, N-CH_2), 48.0 (N-CH_3), 30.4 (N-CH_2-CH_2), 25.3 (N-$(CH_2)_2$-CH_2), 23.0 (CH_2-CH_2-CH_3), 21.7 (CH_2-CH_3), 21.3 (-CH_2-CH_2-), 13.2 ppm (-CH_2-CH_3); IR: $\tilde{v}$ = 741, 827, 892, 915, 936, 970, 998, 1012, 1052, 1238, 1303, 1379, 1408, 1461 (C-H), 2858, 2926, 2957 cm^{-1} (C-H); MS positive mode: m/z (%): 170 [M^+]; MS (40 eV): m/z (%): 86 (100) [$C_5H_{12}N^+$].

A solution of lithium bis(trifluoromethylsulfonyl)imide (140.9 g, 491 mmol) in water (125 mL) was added under stirring to a solution of *N,N*-hexylmethylpyrrolidinium chloride (96.2 g, 468 mmol) in water (120 mL). The reaction mixture was stirred for 24 h at room temperature. Then, dichloromethane (60 mL) was added. The organic layer was separated and washed with water (6 × 100 mL). Subsequently, the organic layer was dried over Na_2SO_4 overnight. The solvent was removed by evaporation in vacuo. The HexMPyrNTf$_2$ was dried in vacuo at 80 °C for 5 days. Yield 83% (176.1 g, 390 mmol), water content: 0.022%; ^1H NMR (300 MHz, CD_3CN, 25 °C, TMS): δ = 3.46–3.41 (m, 4H; CH_2), 3.28–3.23 (m, 2H; CH_2), 2.98 (s, 3H; CH_3), 2.21–2.17 (m, 4H, CH_2), 1.79–1.72 (m, 2H; CH_2), 1.37 (s, 6H; CH_2), 0.94 ppm (t, ^3J(H,H) = 6,7 Hz, 3H; CH_3); ^{13}C NMR (75 MHz, CD_3CN, 25 °C, TMS): δ = 119.9 (q, ^1J(C,F) = 320.7 Hz; CF_3), 64.3 (CH_2-N), 64.2 (CH_2-N), 48.2 (CH_3-N), 30.9 (N-CH_2-CH_2), 25.6 (CH_2-CH_2-CH_3), 23.2 (CH_2-CH_2-CH_3), 22.1 (CH_2-CH_3), 21.3 (CH_2-CH_2), 13.2 ppm (CH_2-CH_3); IR: $\tilde{v}$ = 740, 761, 788, 1052 1133, 1177, 1225, 1329 (S=O), 1347, 1468 (C-H), 2864, 2935, 2961 cm^{-1} (C-H); MS negative mode: m/z (%): 280 (100) [M^-], 147 (24) [$CF_3NO_2S^-$]; MS positive mode (35 eV): m/z (%): 171 (16) [$M^+ + H$], 170 (100) [M^+], 86 (64) [$C_5H_{12}N^+$]. DSC measurements using cooling and heating rates of 1 K min^{-1} showed T_g at −86.5 °C, $T_{recryst}$ at −30.2 °C, and T_m at −23.6 °C during heating. The refractive index was 1.4252 at 25 °C and the density was 1.274 g cm^{-3} at 25 °C.

HepMPyrNTf$_2$

N-Methylpyrrolidine (172.0 g, 2.0 mol) was dissolved in isopropanol (210 mL) and 1-chloroheptane (300.0 g, 2.2 mol) was added dropwise at 3 °C for 1.5 h. After the reaction mixture was stirred for 24 h at 82 °C, the mixture was cooled to room temperature. The solid HepMPyrCl was dried and transferred into a column used for column chromatography. Extraction of HepMPyrCl was carried out with ethyl acetate (800 mL) at one drop per 4 s dropping rate. The purified HepMPyrCl was isolated and dried in vacuo at 40 °C and 3 mbar. Yield: 40% (177.8 g, 809 mmol); m.p. 180 °C; ^1H NMR (300 MHz, D_2O, 25 °C, TMS): δ = 3.43–3.41 (m, 4H; CH_2), 3.26–3.21

(m, 2H; CH$_2$), 2.95 (s, 3H; CH$_3$), 2.21 (s, 4H; CH$_2$), 1.74–1.69 (m, 2H; CH$_2$), 1.28–1.21 (m, 8H; CH$_2$), 0.79 ppm (t, ^3J(H,H) = 6.7 Hz, 3H; CH$_3$); ^{13}C NMR (75 MHz, D$_2$O, 25 °C, TMS): δ = 64.3–64.1 (m, N-CH$_2$), 48.1–47.9 (m, N-CH$_3$), 30.7 (N-CH$_2$-CH$_2$), 27.8 (N-(CH$_2$)$_2$-CH$_2$), 25.6 (N-(CH$_2$)$_3$-CH$_2$), 23.0 (CH$_2$-CH$_2$-CH$_3$), 21.8 (CH$_2$-CH$_3$), 21.3 (CH$_2$-CH$_2$), 13.3 ppm (CH$_2$-CH$_3$); IR: $\tilde{v}$ = 726, 819, 912, 933, 957, 1002, 1050, 1105, 1134, 1160, 1236, 1301, 1341, 1374, 1392, 1462 (C-H), 2857, 2925, 2959 cm^{-1} (C-H); MS positive mode: m/z (%): 184 (100) [M^+]; MS (35 eV): m/z (%): 184 (42) [M^+], 86 (100) [C$_5$H$_{12}$N$^+$].

A solution of lithium bis(trifluoromethylsulfonyl)imide (105.8 g, 368 mmol) in water (100 mL) was added under stirring to a solution of N,N-heptylmethylpyrrolidinium chloride (77.1 g, 351 mmol) in water (70 mL). After the reaction mixture was stirred for 24 h at room temperature, dichloromethane (100 mL) was added. The organic layer was separated and washed with water (4×70 mL). Subsequently, the organic layer was dried over Na$_2$SO$_4$ overnight. The solvent was removed by evaporation. The HepMPyrNTf$_2$ was dried for 24 h in vacuo at 50 °C. Yield: 77% (125.3 g, 270 mmol), water content: 0.083%; ^{1}H NMR (300 MHz, CD$_3$CN, 25 °C, TMS): δ = 3.46–3.41 (m, 4H; CH$_2$), 3.28–3.22 (m, 2H; CH$_2$), 2.97 (s, 3H; CH$_3$), 2.21–2.17 (m, 4H; CH$_2$), 1.82–1.72 (m, 2H; CH$_2$), 1.39–1.35 (m, 8H; CH$_2$), 0.94 ppm (t, ^3J(H,H) = 6.7 Hz, 3H; CH$_3$); ^{13}C NMR (75 MHz, CD$_3$CN, 25 °C, TMS): δ = 119.9 (q, ^1J(C,F) = 320.8 Hz, CF$_3$), 64.3 (N-CH$_2$), 48.2 (N-CH$_3$), 31.2 (CH$_2$), 28.4 (CH$_2$), 25.9 (CH$_2$), 23.2 (CH$_2$), 22.2 (CH$_2$), 21.3 (CH$_2$), 13.3 ppm (CH$_2$-CH$_3$); IR: $\tilde{v}$ = 739, 762, 788, 930, 1053, 1134, 1178, 1225, 1330 (S=O), 1348, 1468 (C-H), 2862, 2932 cm^{-1} (C-H); MS positive mode (40 eV): m/z (%): 184 (10) [M^+], 86 (100) [C$_5$H$_{12}$N$^+$]; MS negative mode (35 eV): m/z (%): 280 (20) [M^-], 211 (74) [CF$_3$NO$_4$S$_2^-$], 147 (100) [CF$_3$NO$_2$S$^-$]. DSC measurements using cooling and heating rates of 5 K min^{-1} showed T_g at −85.3 °C during heating. The refractive index was 1.4277 at 25 °C and the density was 1.279 g cm^{-3}.

OctMPyrNTf$_2$

N-Methylpyrrolidine (165.4 g, 1.9 mol) was dissolved in isopropanol (160 mL) and 1-chlorooctane (308.4 g, 2.0 mol) was added dropwise at 4 °C for 1.5 h. After the reaction mixture was stirred for 24 h at 82 °C, the mixture was cooled to room temperature. The residual solid was washed seven times with ethyl acetate (200 mL). Subsequently, the solvent was removed by evaporation. Yield: 20% (86.5 g, 370 mmol); m.p. 185 °C; ^{1}H NMR (300 MHz, D$_2$O, 25 °C, TMS): δ = 3.50–3.38 (m, 4H; CH$_2$), 3.30–3.25 (m, 2H; CH$_2$), 2.99 (s, 3H; CH$_3$), 2.16 (s, 4H; CH$_2$), 1.77–1.72 (m, 2H; CH$_2$), 1.31–1.24 (m, 10H; CH$_2$), 0.83 ppm (t, ^3J(H,H) = 6,6 Hz, 3H; CH$_3$); ^{13}C NMR (75 MHz, D$_2$O, 25 °C, TMS): δ = 64.3 (N-CH$_2$), 48.1 (N-CH$_3$), 31.2 (CH$_2$), 28.4 (CH$_2$), 28.4 (CH$_2$), 25.8 (CH$_2$), 23.2 (CH$_2$), 22.2 (CH$_2$), 21.3 (CH$_2$-CH$_2$), 13.6 ppm (CH$_2$-CH$_3$); IR: $\tilde{v}$ = 724, 913, 932, 960, 1003, 1046, 1304, 1378, 1407, 1463 (C-H), 2854, 2923, 2957 cm^{-1}(C-H); MS positive mode (35 eV): m/z (%): 86 (100) [C$_5$H$_{12}$N$^+$]; MS: m/z (%): 198 (100) [M^-].

A solution of lithium bis(trifluoromethylsulfonyl)imide (111.5 g, 388 mmol) in water (100 mL) was added under stirring to a solution of N,N-octylmethylpyrrolidinium chloride (86.50 g, 370 mmol) dissolved in water (100 mL). After the reaction mixture was stirred for 24 h at room temperature, dichloromethane (120 mL) was added. The organic layer was separated and washed with water (7× 100 mL). Subsequently, the organic layer was dried over Na$_2$SO$_4$ overnight. The solvent was removed by evaporation. The OctMPyrNTf$_2$ was dried in vacuo at 80 °C for 5 days. Yield: 86% (152.5 g, 390 mmol), water content: 0.033%; ^{1}H NMR (300 MHz, CD$_3$CN, 25 °C, TMS): δ = 3.46–3.41 (m, 4H; CH$_2$), 3.28–3.23 (m, 2H; CH$_2$), 2.98 s, 3H; CH$_3$), 2.19 (s, 4H; CH$_2$), 1.82–1.74 (m, 2H; CH$_2$), 1.37–

1.34 (m, 10H; CH$_2$), 0.93 ppm (t, ^3J(H,H) = 6.7 Hz, 3H; CH$_3$); ^{13}C NMR (75 MHz, CD$_3$CN, 25 °C, TMS): δ = 119.9 (q, ^1J(C,F) = 320.8 Hz; CF$_3$), 64.2 (N-CH$_2$), 48.2 (N-CH$_3$), 31.4 (CH$_2$), 28.7 (CH$_2$), 28.7 CH$_2$), 25.9 (CH$_2$), 23.3 (CH$_2$), 22.3 (CH$_2$), 21.3 (CH$_2$-CH$_2$), 13.4 ppm (CH$_2$-CH$_3$); IR: $\tilde{v}$ = 739, 762, 788, 931, 1053, 1134, 1179, 1225, 1329 (S=O), 1348, 1468 (C-H), 2860, 2930 cm^{-1} (C-H); MS negative mode: m/z (%): 280 (100) [M^-], 147 (24) [CF$_3$NO$_2$S$^-$]; MS positive mode (35 eV): m/z (%): 199 (18) [M^++H], 198 (88) [M^+], 86 (100) [C$_5$H$_{12}$N$^+$]. DSC measurements using cooling and heating rates of 5 K min^{-1} showed T_g at −82.9 °C, $T_{recryst}$ at −34.1 °C (broad peak), T_{m1} at −17.9 °C, and T_{m2} at −12.2 °C during heating. The refractive index was 1.4288 at 25 °C and the density was 1.192 g cm^{-3}.

NonMPyrNTf$_2$

N-Methylpyrrolidine (51.5 g, 605 mol) was dissolved in isopropanol (70 mL) and 1-chlorononane (108.5 g, 647 mol) was added dropwise at room temperature for 1.5 h. After the reaction mixture was stirred for 72 h at 100 °C, the mixture was cooled to room temperature and the isopropanol was removed by evaporation. The residual solid was taken into a column and washed with ethyl acetate (1.5 L) at one drop per 4 s dropping rate. The product was washed and subsequently dried in vacuo. Yield: 76% (113.5 g, 458 mmol); m.p. 183 °C; ^{1}H NMR (300 MHz, CD$_3$CN, TMS): δ = 3.74–3.56 (m, 14; 2×N-CH$_2$), 3.57–3.44 (m, 2H; N-CH$_2$), 3.13 (s, 3H; N-CH$_3$), 2.17 (s, 4H; CH$_2$-CH$_2$), 1.84–1.62 (m, 2H; N-CH$_2$-CH$_2$), 1.45–1.15 (m, 12H; CH$_2$-(CH$_2$)$_6$-CH$_3$), 0.89 ppm (t, ^3J(H,H) = 6.7 Hz; 3H, CH$_3$); ^{13}C NMR (75 MHz, CD$_3$CN, 25 °C, TMS): δ = 64.5 (2×N-CH$_2$), 64.2 (N-CH$_2$), 48.5 (N-CH$_3$), 32.4 (N-CH$_2$-CH$_2$), 29.9 (N-(CH$_2$)$_2$-CH$_2$), 29.7 (N-(CH$_2$)$_3$-CH$_2$), 29.6 (N-(CH$_2$)$_4$-CH$_2$), 26.9 (CH$_2$-(CH$_2$)$_2$-CH$_3$), 24.2 (CH$_2$-CH$_2$-CH$_3$), 23.2 (CH$_2$-CH$_3$), 22.0 (N-CH$_2$-CH$_2$-N), 14.3 ppm (-CH$_2$-CH$_3$); IR: $\tilde{v}$ = 588, 619, 723, 826, 911, 934, 1005, 1235, 1303, 1378, 1464, 1750, 2854, 2922, 2955 cm^{-1}; MS: m/z (%): 212 (100) [M^+]; MS (40 eV): m/z (%): 86 (100) [C$_5$H$_{12}$N$^+$], 212 (10) [M^+].

A solution of lithium bis(trifluoromethysulfonyl)imide (93.3 g, 325 mmol) in water (50 mL) was added under stirring to a solution of N,N-nonylmethylpyrrolidinium chloride (74.6 g, 301 mmol) dissolved in water (250 mL). After the reaction mixture was stirred at room temperature for 72 h, dichloromethane (80 mL) was added and the organic layer was washed with water (6×50 mL). Subsequently, the organic layer was dried over Na$_2$SO$_4$ overnight, and the solvent was removed by evaporation in vacuo. The product was dried in vacuo at room temperature for 1 day. Yield 99% (146.1 g, 297 mmol), water content: 0.023%; ^{1}H NMR (300 MHz, CDCl$_3$, 25 °C, TMS): δ = 3.48 (t, ^3J(H-H) = 5.5 Hz; 4H, 2×N-CH$_2$), 3.35–3.19 (m, 2H; N-CH$_2$), 3.01 (s, 3H; N-CH$_3$), 2.25 (m, 4H; CH$_2$-CH$_2$), 1.75 (m, 2H; N-CH$_2$-CH$_2$), 1.45–1.16 (m, 12H; CH$_2$-(CH$_2$)$_6$-CH$_3$), 0.88 ppm (t, 1 J(H-H) = 6.6 Hz; 3H, CH$_3$); ^{13}C NMR (75 MHz, CDCl$_3$, 25 °C, TMS): δ = 119.9 (q, ^1J(C,F) = 319 Hz, CF$_3$), 64.8 (N-CH$_2$), 64.4 (N-CH$_2$), 48.2 (N-CH$_3$), 31.7 (N-CH$_2$-CH$_2$), 29.2 (N-(CH$_2$)$_2$-CH$_2$), 29.0 (N-(CH$_2$)$_3$-CH$_2$), 28.9 (N-(CH$_2$)$_4$-CH$_2$), 26.1 (CH$_2$-(CH$_2$)$_2$-CH$_3$), 23.7 (CH$_2$-CH$_2$-CH$_3$), 22.6 (CH$_2$-CH$_3$), 21.4 (N-CH$_2$-CH$_2$-N), 14.0 ppm (-CH$_2$-CH$_3$); IR: $\tilde{v}$ = 511, 569, 600, 614, 653, 739, 762, 788, 932, 1052, 1133, 1177, 1225, 1330, 1348, 1467, 2858, 2928 cm^{-1}; MS (35 eV): m/z (%): 212 (100) [M^+], 86 (100) [C$_5$H$_{12}$N$^+$], 212 (17) [M^+]; MS: m/z (%): 280 (100) [M^-]. DSC measurements using cooling and heating rates of 5 K min^{-1} showed T_g at −80.8 °C, $T_{recryst}$ at −34.9 °C, T_{m1} at −8.1 °C, and T_{m2} at −4.6 °C during heating. The refractive index was 1.4307.

DecMPyrNTf$_2$

N-Methylpyrrolidine (93.7 g, 1.1 mol) was dissolved in isopropanol (120 mL) and 1- chlorodecane (207.5 g, 2.2 mol) was added drop-

wise at 3 °C for 1.5 h. After the reaction mixture was stirred at 82 °C for 34 h, the mixture was cooled to room temperature. The residual solid was washed ten times with ethyl acetate (400 mL). Subsequently, the solvent was removed by evaporation. Yield: 25 % (69.7 g, 280 mmol); m.p. 162 °C; ^{1}H NMR (300 MHz, D$_2$O, 25 °C, TMS): $\delta = 3.50$–3.30 (m, 4H; CH$_2$), 3.28–3.24 (m, 2H; CH$_2$), 2.99 (s, 3H; CH$_3$), 2.16 (s, 4H; CH$_2$), 1.74–1.72 (m, 2H; CH$_2$), 1.30–1.23 (m, 14H; CH$_2$), 0.82 ppm (t, ^{3}J(H,H) = 6.6 Hz, 3H; CH$_3$); ^{13}C NMR (75 MHz, D$_2$O, 25 °C, TMS): $\delta = 64.1$ (N-CH$_2$), 48.1 (N-CH$_3$), 31.6 (N-CH$_2$-*CH$_2$*), 29.2 (N-CH$_2$-CH$_2$-*CH$_2$*), 29.0 (*CH$_2$*-CH$_2$-(CH$_2$)$_4$-CH$_3$), 28.7 (*CH$_2$*-(CH$_2$)$_3$-CH$_3$), 26.0 (*CH$_2$*-(CH$_2$)$_2$-CH$_3$), 23.3 (*CH$_2$*-CH$_2$-CH$_3$), 22.4 (*CH$_2$*-CH$_3$), 21.33 (*CH$_2$*-CH$_2$), 13.8 ppm (CH$_2$-*CH$_3$*); IR: $\tilde{\nu} = 723$, 912, 935, 956, 1007, 1046, 1104, 1160, 1237, 1301, 1372, 1465(C-H), 1740, 2854, 2923, 2957 cm^{-1} (C-H); MS (35 eV): m/z (%): 86 (100) [C$_5$H$_{12}$N$^+$]; MS: m/z (%): 227 (17) [M$^-$ + H], 226 (100) [M$^-$].

A solution of lithium bis(trifluoromethylsulfonyl)imide (84.7 g, 293 mmol) in water (75 mL) was added under stirring to a solution of N,N-decylmethylpyrrolidinium chloride (69.7 g, 280 mmol) in water (75 mL). After the reaction mixture was stirred for 24 h at room temperature, dichloromethane (120 mL) was added. The organic layer was separated and washed with water (4×100 mL). Subsequently, the organic layer was dried over Na$_2$SO$_4$ during 48 h. The solvent was removed by evaporation in vacuo. The product was dried in vacuo at 80 °C for 5 days. Yield: 82 % (116.4 g, 230 mmol), water content: 0.042 %; ^{1}H NMR (300 MHz, CD$_3$CN, 25 °C, TMS): $\delta = 3.48$–3.37 (m, 4H; CH$_2$), 3.28–3.22 (m, 2H; CH$_2$), 2.98 (s, 3H; CH$_3$), 2.19 (s, 4H; CH$_2$), 1.82–1.74 (m, 2H; CH$_2$), 1.37–1.33 (m, 14H; CH$_2$), 0.93 ppm (t, ^{3}J(H,H) = 6.6 Hz, 3H; CH$_3$); ^{13}C NMR (75 MHz, CD$_3$CN, 25 °C, TMS): $\delta = 119.9$ (q, ^{1}J(C,F) = 320.8 Hz; CF$_3$), 64.3 (N-CH$_2$), 48.2 (N-CH$_3$), 31.6 (N-CH$_2$-*CH$_2$*), 29.2 (N-CH$_2$-CH$_2$-*CH$_2$*), 29.0 (*CH$_2$*-CH$_2$-(CH$_2$)$_4$-CH$_3$), 28.7 (*CH$_2$*-(CH$_2$)$_3$-CH$_3$), 26.0 (*CH$_2$*-(CH$_2$)$_2$-CH$_3$), 23.3 (*CH$_2$*-CH$_2$-CH$_3$), 22.4 (*CH$_2$*-CH$_3$), 21.3 (*CH$_2$*-CH$_2$), 13.4 ppm (CH$_2$-*CH$_3$*); IR: $\tilde{\nu} = 739$, 762, 788, 932, 1033, 1053, 1134, 1178, 1225, 1329 (S=O), 1347, 1467 (C-H), 2857, 2927 cm^{-1} (C-H); MS negative mode: m/z (%): 280 (100) [M$^-$], 147 (24) [CF$_3$NO$_2$S$^-$]; MS positive mode (35 eV): m/z (%): 227 (14) [M$^+$ + H], 226 (58) [M$^+$], 86 (100) [C$_5$H$_{12}$N$^+$]. DSC measurements using cooling and heating rates of 5 K min^{-1} showed two exothermic peaks, T_{cryst1} at -19.6 °C and T_{cryst2} at -36.5 °C, during cooling and two endothermic peaks, T_{m1} at -13.6 °C and T_{m2} at 12.6 °C, during heating. The refractive index was 1.4316 at 25 °C and the density was 1.152 g cm^{-3}.

Methods

The ionic liquid solutions were filtered before the measurements were carried out by using a 0.45 μm PTFE filter to avoid scattering of light by nondissolved small precursor particles. UV/Vis spectra of ionic liquids and o-Cl-HABI dissolved either in ionic liquids or in molecular solvents were measured with a Cary 5500 UV/Vis–near-IR absorption spectrometer from Varian. The optical density of the o-Cl-HABI was 0.4 at the irradiation wavelength (365 nm). A Hg–Xe 500 W UV lamp (LOT-Oriel) was used to generate lophyl radicals by irradiation at 365 nm of o-Cl-HABI dissolved in either ionic liquids or molecular solvents. The UV/Vis spectra of the lophyl radicals were obtained with an HR2000+ fiber spectrometer from Ocean Optics, by using the temperature-controlled cuvette holder QPOD (Ocean Optics) equipped with a Peltier element and TC125 temperature controller (Ocean Optics). Irradiation was performed until the equilibrium was reached. Absorption measurements were taken with the HR2000+ fiber spectrometer in a geometric arrangement of 90° relative to the excitation light. Kinetic data were analyzed by using an extinction coefficient of 2000 L mol^{-1} cm^{-1} for the ab-

sorption maximum of the lophyl radicals in the different ionic liquids.[3a]

^{1}H and ^{13}C NMR spectra were recorded on a Bruker Fourier-300 MHz spectrometer by using D$_2$O for the N-alkyl-N-methylpyrrolidinium chlorides and CD$_3$CN for N-alkyl-N-methylpyrrolidinium bis(trifluoromethylsulfonyl)imides. Tetramethylsilane (TMS) was used as internal standard. Infrared spectra were recorded on a Bruker FTIR ALPHA instrument. Electrospray mass spectrometry was carried out on an LXQ linear ion trap from Thermo Scientific in both positive and negative mode by using an electron spray source. The instrumental limit of mass detection was about 50. The melting points were measured with a capillary tube apparatus, Melting Point M-565 from Büchi, and quoted from the visual observation of the completion of the melt. Differential scanning calorimetry (Mettler Toledo DSC 822^e and Netzsch Phoenix DSC 204) was used for glass transition temperature and melting point measurements. Calibration was carried out with indium (164.5 °C), tin (231.9 °C), bismuth (271.6 °C), and zinc (419.7 °C). The samples were measured in an aluminum pan in a temperature range between -120 and 120 °C at cooling and heating rates of 5 K min^{-1}. The water content in the ionic liquids was measured by Karl Fisher analysis using the Metrohm 684 KF coulometer and the reagent Hydranal Coulomat AG, purchased from Riedel de Haën. The viscosity of ionic liquids was measured with an AR550 rheometer (TA Instruments) equipped with a Peltier plate and a 40 mm cone 1° for a sample volume of 0.3 mL and a shear rate of 10 s^{-1}. The refractive index of the synthesized ionic liquids was determined with a digital refractometer (Agato RX-5000 α).

[1] a) T. Hayashi, K. Maeda, *Bull. Chem. Soc. Jpn.* **1960**, *33*, 565–566; b) T. Hayashi, K. Maeda, S. Shida, K. Nakada, *J. Chem. Phys.* **1960**, *32*, 1568; c) H. Zimmermann, H. Baumgärtel, F. Bakke, *Angew. Chem.* **1961**, *73*, 808–808; d) T. Hayashi, K. Maeda, *Bull. Chem. Soc. Jpn.* **1962**, *35*, 2057–2058; e) D. M. White, J. Sonnenberg, *J. Am. Chem. Soc.* **1964**, *86*, 5685–5686; f) D. M. White, J. Sonnenberg, *J. Am. Chem. Soc.* **1966**, *88*, 3825–3829; g) T. Hayashi, K. Maeda, M. Morinaga, *Bull. Chem. Soc. Jpn.* **1964**, *37*, 1563–1564; h) M. A. J. Wilks, M. R. Willis, *Nature* **1966**, *212*, 500–502; i) M. A. J. Wilks, M. R. Willis, *J. Chem. Soc. B* **1968**, 1526–1529; j) K. Maeda, T. Hayashi, *Bull. Chem. Soc. Jpn.* **1970**, *43*, 429–438; k) T. Shida, K. Maeda, T. Hayashi, *Bull. Chem. Soc. Jpn.* **1970**, *43*, 652–657; l) L. A. Cescon, G. R. Coraor, R. Dessauer, E. F. Silversmith, E. J. Urban, *J. Org. Chem.* **1971**, *36*, 2262–2267; m) L. A. Cescon, G. R. Coraor, R. Dessauer, A. S. Deutscher, H. L. Jackson, A. MacLachlan, K. Marcali, E. M. Potrafke, R. E. Read, E. F. Silversmith, E. J. Urban, *J. Org. Chem.* **1971**, *36*, 2267–2272; n) R. H. Riem, A. MacLachlan, G. R. Coraor, E. J. Urban, *J. Org. Chem.* **1971**, *36*, 2272–2275; o) A. MacLachlan, R. H. Riem, *J. Org. Chem.* **1971**, *36*, 2275–2280; p) R. L. Cohen, *J. Org. Chem.* **1971**, *36*, 2280–2284; q) N. Cyr, M. A. J. Wilks, M. R. Willis, *J. Chem. Soc. B* **1971**, 404–406; r) B. S. Tanaseischuk, *Chem. Heterocycl. Compd.* **1972**, *8*, 1173–1180; s) H. Tanino, T. Kondo, K. Okada, T. Goto, *Bull. Chem. Soc. Jpn.*

1972, *45*, 1474–1480; t) D. Lavabre, G. Levy, J. P. Laplante, J. C. Micheau, *J. Phys. Chem.* **1988**, *92*, 16–18; u) H. Sato, K. Kasatani, S. Murakami, *Chem. Phys. Lett.* **1988**, *151*, 97–101; v) X.-Z. Qin, A. Lui, A. D. Trifunac, V. V. Krongauz, *J. Phys. Chem.* **1991**, *95*, 5822–5826; w) Q. Q. Zhu, M. Fink, F. Seitz, S. Schneider, W. Schnabel, *J. Photochem. Photobiol. A* **1991**, *59*, 255–263; x) H. Morita, S. Minagawa, *J. Photopolym. Sci. Technol.* **1992**, *5*, 551–556; y) J. V. Caspar, I. V. Khudyakov, N. J. Turro, G. C. Weed, *Macromolecules* **1995**, *28*, 636–641; z) H. Igarashi, T. Igarashi, M. Sagawa, T. Mori, Y. Kotani, Y. Muroya, Y. Katsumura, T. Yamashita, *J. Photopolym. Sci. Technol.* **2007**, *20*, 757–762.

[2] a) M. Kawano, T. Sano, J. Abe, Y. Ohashi, *J. Am. Chem. Soc.* **1999**, *121*, 8106–8107; b) J. Abe, T. Sano, M. Kawano, Y. Oyashi, M. M. Matsushita, T. Iyoda, *Angew. Chem.* **2001**, *113*, 600–602; *Angew. Chem. Int. Ed.* **2001**, *40*, 580–582; c) A. Kikuchi, T. Iyoda, J. Abe, *Chem. Commun.* **2002**, 1484–1485; d) I. Nakahara, A. Kikuchi, F. Iwahori, J. Abe, *Chem. Phys. Lett.* **2005**, *402*, 107–110; e) Y. Miyamoto, A. Kikuchi, F. Iwahori, J. Abe, *J. Phys. Chem. A* **2005**, *109*, 10183–10188; f) Y. Satoh, Y. Ishibashi, S. Ito, Y. Nagasawa, H. Miyasaka, H. Chosrowjan, S. Taniguchi, N. Mataga, D. Kato, A. Kikuchi, J. Abe, *Chem. Phys. Lett.* **2007**, *448*, 228–231; g) F. Iwahori, S. Hatano, J. Abe, *J. Phys. Org. Chem.* **2007**, *20*, 857–863; h) S. Hatano, J. Abe, *J. Phys. Chem. A* **2008**, *112*, 6098–6103; i) K. Fujita, S. Hatano, D. Kato, J. Abe, *Org. Lett.* **2008**, *10*, 3105–3108; j) H. Miyasaka, Y. Satoh, Y. Ishibashi, S. Ito, Y. Nagasawa, S. Taniguchi, H. Chosrowjan, N. Mataga, D. Kato, A. Kikuchi, J. Abe, *J. Am. Chem. Soc.* **2009**, *131*, 7256–7263; k) Y. Harada, S. Hatano, A. Kimoto, J. Abe, *J. Phys. Chem. Lett.* **2010**, *1*, 1112–1115; l) S. Hatano, K. Sakai, J. Abe, *Org. Lett.* **2010**, *12*, 4152–4155; m) A. Kikuchi, Y. Harada, M. Yagi, T. Ubukata, Y. Yokoyama, J. Abe, *Chem. Commun.* **2010**, *46*, 2262–2264.

[3] a) V. Strehmel, J. F. Wishart, D. E. Polyansky, B. Strehmel, *ChemPhysChem* **2009**, *10*, 3112–3118; b) V. Strehmel, *ChemPhysChem* **2012**, *13*, 1649–1663.

[4] a) R. Dessauer, *Adv. Photochem.* **2005**, *28*, 129–261; b) R. Dessauer, *Photochemistry, History and Commercial Applications of Hexaarylbiimidazoles*, Elsevier, Amsterdam, **2006**.

[5] a) B. M. Monroe, G. C. Weed, *Chem. Rev.* **1993**, *93*, 435–448; b) G. Fang, X. Jinqi, Y. Yongyuan, *J. Photopolym. Sci. Technol.* **1999**, *12*, 339–342; c) X. Allonas, J. P. Fouassier, M. Kaji, M. Miyasaka, T. Hidaka, *Polymer* **2001**, *42*, 7627–7632.

[6] a) P. Kubisa, *Prog. Polym. Sci.* **2009**, *34*, 1333–1347; b) V. Strehmel, *Chem. Ing. Tech.* **2011**, *83*, 1443–1453.

[7] a) C. P. Fredlake, J. M. Crosthwaite, D. G. Hert, S. N. V. K. Aki, J. F. Brennecke, *J. Chem. Eng. Data* **2004**, *49*, 954–964; b) V. Strehmel, A. Laschewsky, H. Wetzel, H. Görnitz, *Macromolecules* **2006**, *39*, 923–930; c) M. E. Kandil, K. N. Marsh, A. R. H. Goodwin, *J. Chem. Eng. Data* **2007**, *52*, 2382–2387; d) R. Lungwitz, V. Strehmel, S. Spange, *New J. Chem.* **2010**, *34*, 1135–1140.

[8] a) J.-M. Lee, J. M. Prausnitz, *Chem. Phys. Lett.* **2010**, *492*, 55–59; b) N. D. Khupse, A. Kumar, *J. Phys. Chem. B* **2010**, *114*, 376–381; c) H. Jin, G. A. Baker, S. Arthantsev, J. Dong, M. Maroncelli, *J. Phys. Chem. B* **2007**, *111*, 7291–7302.

[9] O. O. Okoturo, T. J. Vander Noof, *J. Electroanal. Chem.* **2004**, *568*, 167–181.

[10] M. A. Saleh, O. Ahmed, M. S. Ahmed, *J. Mol. Liq.* **2004**, *115*, 41–47.

[11] T. Asano, *Pure Appl. Chem.* **1999**, *71*, 1691–1704.

[12] a) A. K. Burrell, R. E. Del Sesto, S. N. Baker, T. M. McCleskeya, G. A. Baker, *Green Chem.* **2007**, *9*, 449–454; b) B. R. Clare, P. M. Bayley, A. S. Best, M. Forsyth, D. R. MacFarlane, *Chem. Commun.* **2008**, 2689–2691.

[13] a) S. Spange, R. Sens, Y. Zimmermann, H. Seifert, I. Roth, S. Anders, K. Hofmann, *New. J. Chem.* **2003**, *27*, 520–524; b) D. M. Alonso, M. L. Gramados, R. Mariscal, A. Donhal, *J. Catal.* **2009**, *262*, 18–26.

[14] a) V. Strehmel, H. Rexhausen, P. Strauch, E. Görnitz, B. Strehmel, *ChemPhysChem* **2008**, *9*, 1294–1302; b) V. Strehmel, H. Rexhausen, P. Strauch, B. Strehmel, *ChemPhysChem* **2010**, *11*, 2182–2190.

[15] S. H. Chung, R. Lopato, S. G. Greenbaum, H. Shirota, E. W. Castner, J. F. Wishart, *J. Phys. Chem. B* **2007**, *111*, 4885–4893.